On-line optical imaging of the human brain with 160-ms temporal resolution

Maria Angela Franceschini

Bioengineering Center, Department of Electrical Engineering and Computer Science
Tufts University, 4 Colby Street, Medford, MA 02155

mari@EECS.TUFTS.EDU

http://www.eotc.tufts.edu/Documents/Faculty/Franceschini/index.html

Vlad Toronov, Mattia E. Filiaci, Enrico Gratton

Laboratory for Fluorescence Dynamics, University of Illinois at Urbana-Champaign,
1110 West Green Street, Urbana, IL 61801

ENRICO@SCS.UIUC.EDU

Sergio Fantini

Bioengineering Center, Department of Electrical Engineering and Computer Science
Tufts University, 4 Colby Street, Medford, MA 02155

Sergio.Fantini@TUFTS.EDU

Abstract: We have developed an instrument for non-invasive optical imaging of the human brain that produces on-line images with a temporal resolution of 160 ms. The imaged quantities are the temporal changes in cerebral oxy-hemoglobin and deoxy-hemoglobin concentrations. We report real-time videos of the arterial pulsation and motor activation recorded on a 4×9 cm^2 area of the cerebral cortex in a healthy human subject. This approach to optical brain imaging is a powerful tool for the investigation of the spatial and temporal features of the optical signals collected on the brain.

OCIS codes: (170.3880) Medical and biological imaging; (170.0110) Imaging systems; (170.1470) Blood/tissue constituent monitoring

References and links

1. S. P. Gopinath, C. S. Robertson, R. G. Grossman, and B. Chance, "Near-Infrared Spectroscopic Localization of Intracranial Hematomas," J. Neurosurg. **79**, 43-47 (1993).
2. Y. Hoshi, S. Mizukami, M. Tamura, "Dynamic features of hemodynamic and metabolic changes in the human brain during all-night sleep revealed by near-infrared spectroscopy," Brain Research **652**, 257-262 (1994).
3. Y. Hoshi, M. Tamura, "Fluctuations in the cerebral oxygenation state during the resting period in functional mapping studies of the human brain," Med. Biol. Eng. Comput. **35**, 328-330 (1997).
4. A. Villringer, J. Planck, C. Hock, L. Schleinkofer, and U. Dirnagl, "Near Infrared Spectroscopy (NIRS): A New Tool to Study Hemodynamic Changes During Activation of Brain Function in Human Adults," Neurosci. Lett. **154**, 101-104 (1993).
5. A. Maki, Y. Yamashita, Y. Ito, E. Watanabe, Y. Mayanagi, H. Koizumi, "Spatial and temporal analysis of human motor activity using noninvasive NIR topography," Med. Phys. **22**, 1997-2005 (1995).
6. G. Gratton, M. Fabiani, D. Friedman, M. A. Franceschini, S. Fantini, P. M. Corballis, and E. Gratton, "Rapid Changes of Optical Parameters in the Human Brain During a Tapping Task," J. Cognitive Neuroscience **7**, 446-456 (1995).
7. H. Obrig, C. Hirth, J. G. Junge-Hülsing, C. Döge, T. Wolf, U. Dirnagl, A. Villringer, "Cerebral oxygenation changes in response to motor stimulation," J Appl. Physiol. **81**, 1174-1183 (1996).
8. B. Chance, Z. Zhuang, C. UnAh, and L. Lipton, "Cognition-activated low-frequency modulation of light absorption in human brain," Proc. Natl. Acad. Sci. USA **90**, 3770-3774 (1993).

#18957 - $15.00 US
Received December 14, 1999; Revised January 19, 2000

9. Y. Hoshi and M. Tamura, “Detection of Dynamic Changes in Cerebral Oxygenation Coupled to Neuronal Function During Mental Work in Man,” Neurosci. Lett. **150**, 5-8 (1993).

10. T. Kato, A. Kamei, S. Takashima, T. Ozaki, “Human visual cortical function during photic stimulation monitoring by means of near-infrared spectroscopy,” J Cereb. Blood Flow Metab. **13**, 516-520 (1993).

11. J. H. Meek, C. E. Elwell, M. J. Khan, J. Romaya, J. S. Wyatt, D. T. Delpy, and S. Zeki, “Regional Changes in Cerebral Haemodynamics as a Result of a Visual Stimulus Measured by Near Infrared Spectroscopy,” Proc. Roy. Soc. London B **261**, 351-356 (1995).

12. H. R. Heekeren, H. Obrig, H. Wenzel, R. Eberle, J. Ruben, K. Villringer, R. Kurth and A. Villringer, “Cerebral haemoglobin oxygenation during substained visual stimulation – a near-infrared spectroscopy study,” Proc. R Soc. Lond. B **352**, 743-750 (1997).

13. A. M. Siegel, J. J. A. Marota, and D. Boas, “Design and evaluation of a continuous-wave diffuse optical tomography system,” Opt. Express **4**, 287-298 (1999). http://epubs.osa.org/opticsexpress/tocv4n8.htm

14. B. Chance, E. Anday, S. Nioka, S. Zhou, L. Hong, K. Worden, C. Li, T. Murray, Y. Ovetsky, D. Pidikiti and R. Thomas, “A novel method for fast imaging of brain function, non-invasively, with light,” Opt. Express **2**, 411-423 (1998). http://epubs.osa.org/opticsexpress/framestocv2n10.htm

15. R. M. Danen, Y. Wang, X. D. Li, W. S. Thayer and A. G. Yodh, “Regional imager for low-resolution functional imaging of the brain with diffusing near-infrared light,” Photochem. Photobiol. **67**, 33-40 (1998).

16. S. R. Hintz, D. A. Benaron, J. P. van Houten, J. L. Duckworth, F. W. H. Liu, S. D. Spilman, D. K. Stevenson and W.-F. Cheong, “Stationary headband for clinical time-of-flight optical imaging at the bedside,” Photochem. Photobiol. **68**, 361-369 (1998).

17. S. R. Hintz, W.-F. Cheong, J. P. van Houten, D. K. Stevenson and D. A. Benaron, “Bedside imaging of intracranial hemorrhage in the neonate using light: Comparison with ultrasound, computed tomography, and magnetic resonance imaging,” Pediatr. Res. **45**, 54-59 (1999).

18. J. P. van Houten, D. A. Benaron, S. Spilman and D. K. Stevenson, “Imaging brain injury using time-resolved near infrared light scanning,” Pediatr. Res. **39**, 470-476 (1996).

19. Y. Shinohara, M. Haida, N. Shinohara, F. Kawaguchi, Y. Itoh and H. Koizumi, “Towards near-infrared imaging of the brain,” Adv. Exp. Med. Biol. **413**, 85-89 (1997).

20. C. Hirth, K. Villringer, A. Thiel, J. Bernarding, W. Mühlnickl, H. Obrig, U. Dirnagl and A. Villringer, “Towards brain mapping combining near-infrared spectroscopy and high resolution 3D MRI,” Adv. Exp. Med. Biol. **413**, 139-147 (1997).

21. H. Koizumi, Y. Yamashita, A. Maki, T. Yamamoto, Y. Ito, H. Itagaki, and R. Kennan, “Higher-order brain function analysis by trans-cranical dynamic near-infrared spectroscopy imaging,’ J. Biomed. Opt. **4**, 403-413 (1999).

22. S. Fantini, M. A. Franceschini, E. Gratton, D. Hueber, W. Rosenfeld, D. Maulik, P. G. Stubblefield, and M. R. Stankovic, “Non-invasive optical mapping of the piglet brain in real time," Opt. Express **4**, 308-314 (1999). http://epubs.osa.org/opticsexpress/tocv4n8.htm

23. S. Fantini, M. A. Franceschini, J. S. Maier, S. A. Walker, B. Barbieri, and E. Gratton, “Frequency-Domain Multichannel Optical Detector for non-Invasive Tissue Spectroscopy and Oximetry,” Opt. Eng. **34**, 32-42 (1995).

24. M. A. Franceschini, D. Wallace, B. Barbieri, S. Fantini, W. W. Mantulin, S. Pratesi, G. P. Donzelli, and E. Gratton, “Optical Study of the Skeletal Muscle During Exercise with a Second Generation Frequency-Domain Tissue Oximeter,” Proc. SPIE **2979**, 807-814 (1997).

25. M. Cope and D. T. Delpy, “System for long-term measurement of cerebral blood and tissue oxygenation on newborn infants by near infrared transillumination,” *Med. Biol. Eng. Comput.* **26**, 289-294 (1988).

26. A. Duncan, J. H. Meek, M. Clemence, C. E. Elwell, L. Tyszczuk, M. Cope, D. T. Delpy, “Optical pathlenght measurements on adult head, calf and forearm and the head of the newborn infant using phase resolved optical spectroscopy,” Phys. Med. Biol.. **40**, 295-304 (1995).

27. E. M. Sevick, B. Chance, J. Leigh, S. Nioka and M. Maris, “Quantitation of time- and frequency-resolved optical spectra for the determination of tissue oxygenation,” Anal. Biochem. **195**, 330-351 (1991).

28. C. Hirth, H. Obrig, J. Valdueza, U. Dirnagl, and A. Villringer, “Simultaneous assessment of cerebral oxygenation and hemodynamics during a motor task,” in *Oxygen Transport to Tissue XVIII*, edited by E. M. Nemoto and J. C. LaManna (Plenum Press, New York, NY, 1997), pp. 461-469.

29. V. Toronov, M. A. Franceschini, M. Filiaci, M. Wolf, S. Fantini, and E. Gratton, “Near-Infrared Study of Fluctuations in Cerebral Hemodynamics During Rest and Motor Stimulation: Spatial Mapping and Temporal Analysis,” Med. Phys. (submitted).

30. M. Kohl, C. Nolte, H. R. Heekeren, S. Horst, U. Scholz, H. Obrig, and A. Villringer, “Determination of the wavelength dependence of the differential pathlength factor from near-infrared pulse signals,” Phys. Med. Biol. **43**, 1771-1782 (1998).

#18957 - $15.00 US Received December 14, 1999; Revised January 19, 2000

31. G. Gratton, P. M. Corballis, E. Cho, M. Fabiani, and D. C. Hood, "Shades of Gray Matter: Noninvasive Optical Images of Human Brain Responses During Visual Stimulation," Psychophysiology **32**, 505-509 (1995).

32. M. A. Franceschini, S. Fantini, L. A. Paunescu, J. S. Maier, and E. Gratton, "Influence of a Superficial Layer in the Quantitative Spectroscopic Study of Strongly Scattering Media," Appl. Opt. **37**, 7447-7458 (1998).

33. M. A. Franceschini, E. Gratton, and S. Fantini, "Non-Invasive Optical Method to Measure Tissue and Arterial Saturation: an Application to Absolute Pulse Oximetry of the Brain," Opt. Lett. **24** (12), 829-831 (1999).

1. Introduction

Near-infrared spectroscopy (NIRS) is an effective technique for the non-invasive monitoring of cerebral hemodynamics and oxygenation. A number of studies have shown the non-invasive applicability of optical techniques to the detection of intracranial hematomas [1], the monitoring of cerebral hemodynamics during sleep [2,3], and the study of the activation of the motor [4-7], cognitive [8,9] and visual [10-12] cortex in human subjects. Optical imaging of the brain, where the temporal information provided by NIRS is spatially resolved, shows promise as an alternative to functional magnetic resonance imaging (fMRI) and positron emission tomography (PET). Most of the devices for optical brain imaging feature relatively long acquisition times. In fact, reported acquisition times per image are 3-5 s [5,13], < 30 s [14], 2.5 min [15], several hours [16,17], 1-3 days [18], and not-quantified "slow data acquisition rate" [19], and "long measurement times" [20]. While these acquisition times can be appropriate for structural imaging or for the monitoring of slow dynamic processes, it is desirable to exploit the capability of high temporal resolution afforded by optical methods in functional brain imaging. In this direction, Koizumi *et al*. [21] have developed a trans-cranial optical imaging device with a quasicontinuous image acquisition at a rate of 2 Hz (acquisition time per image: 500 ms). We have recently reported a fast imaging system that was capable of acquiring optical images of a piglet brain at a rate of 5.21 Hz (acquisition time per image: 192 ms) [22]. In this article, we present a modified version of our imaging system that acquires optical images of a 9 cm $\times$ 4 cm area of the human brain cortex at a rate of 6.25 Hz (acquisition time per image: 160 ms). An acquisition rate faster than twice the heart rate allows us to image the arterial pulsation. The back-projection scheme used by us for image reconstruction is straightforward and can be applied on-line for the display of images in real-time during the measurement. We report three real-time videos of non-invasive optical imaging of the human brain. The first one is the mapping of the arterial pulsation at rest; the second and the third videos report the spatially-resolved hemodynamics observed on the primary motor cortex during contralateral hand tapping.

2. Instrumentation

The basic optical unit is a multi-channel frequency-domain tissue spectrometer [23,24] (ISS, Champaign, IL, Mod. No. 96208). This instrument features sixteen intensity-modulated laser diodes and two heterodyned photomultiplier tube detectors (PMT's). The modulation frequency of the laser intensity is 110 MHz, and the cross-correlation frequency for heterodyne detection is 5 kHz. The sixteen laser diodes and the two PMT's are coupled to optical fibers. The sixteen source fibers (eight guiding light at 758 nm, and eight at 830 nm) are multimode glass fibers 400 μm in core diameter, and the two detector fiber bundles have an internal diameter of 3 mm. The source fiber locations (numbered from 1 to 8) and the detector fibers (labeled as A and B) were placed on the head according to the arrangement shown in Fig. 1. Each source location represents two source optical fibers, one per each wavelength. The source-detector distance on the subject's head between source locations 1, 2, 6, 7, 8 (2, 3, 4, 5, 6) and detector A (B) has the same value of 3.0 cm. This guarantees that each source-detector pair provides a similar optical penetration depth into the brain cortex. The sixteen laser diodes are electronically multiplexed at a rate of 100 Hz (10 ms on-time per

#18957 - $15.00 US Received December 14, 1999; Revised January 19, 2000

diode) to time-share the two parallel PMT detectors. Consequently, the acquisition time for the whole series of 32 source-detector pairs is 160 ms.

Simultaneously with the measurement of frequency-domain optical data on the subject's head, we continuously collected the heart rate (beats per min) of the subject with a pulse oximeter (Nellcor N-200) on a toe.

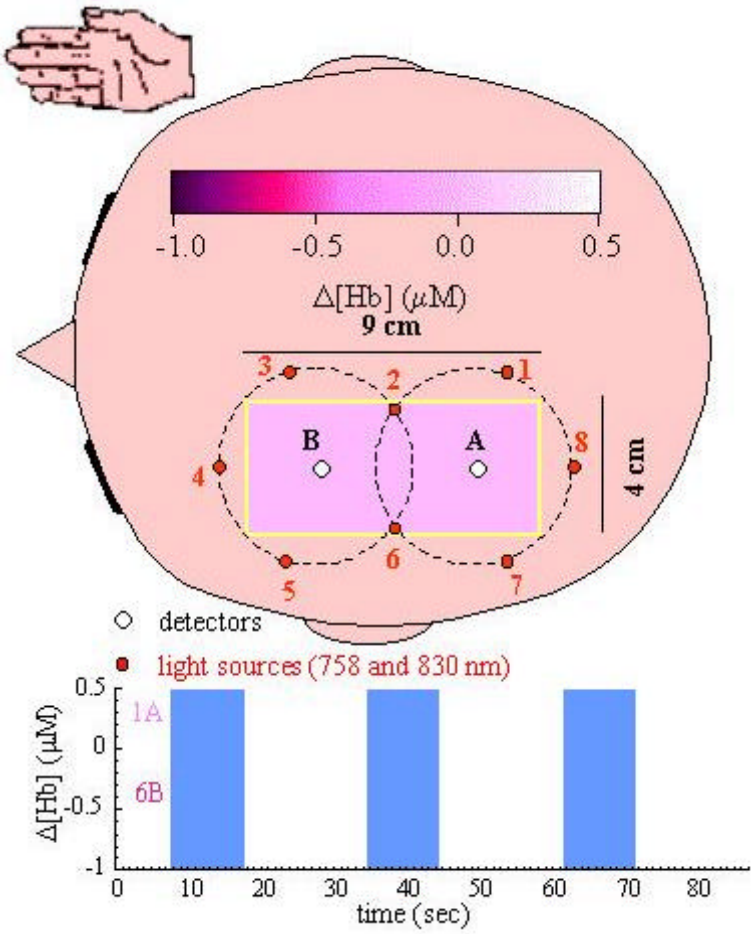

Fig. 1. Geometrical arrangement of the sixteen source optical fibers and two detector fiber bundles on the head of a human subject. Each one of the eight closed circles (numbered 1-8) represents one pair of source fibers at 758 and 830 nm. The two open circles (labeled as A and B) represent the two detector fiber bundles. The rectangle inside the head is the 4×9 cm^2 imaged area. The measurement protocol involves hand-tapping with the right hand (contralateral to the imaged brain area). The 10-s tapping periods are indicated by the blue bars in the temporal diagram. The video displays the real-time evolution of the relative deoxy-hemoglobin concentration (Δ[Hb]) map during the hand-tapping protocol, as well as the temporal traces from two representative source-detector pairs (1A and 6B). Duration of the animated gif video: 87 s; file size: 849 kB.

3. Data processing

We have translated the temporal changes in the intensity measured by each source-detector pair into changes in the absorption coefficient ($\Delta\mu_a$) by using the differential-pathlength-factor (DPF) method [25]. We assumed DPF values of 6.53 at 758 nm and 5.86 at 830 nm on the

#18957 - $15.00 US
Received December 14, 1999; Revised January 19, 2000

basis of literature data [26]. From the values of $\Delta\mu_a$ at two wavelengths, we have calculated the temporal changes in the cerebral oxy-hemoglobin ($\Delta[HbO_2]$) and deoxy-hemoglobin ($\Delta[Hb]$) concentrations [27]. Even though the DPF method yields quantitative concentration changes, the accuracy of the DPF method for non-uniform absorption changes it is limited.

The two-dimensional optical maps are computed by back-projecting the hemoglobin changes measured at each source-detector pairs. The back-projection scheme is illustrated in the matrix on Fig. 2. The pixel size is 0.5 cm × 0.5 cm. The numbers in each pixel indicate the corresponding source location, while their colors indicate the detector (red for detector A, blue for detector B). The value at each image pixel is a linear combination of the readings from no more than three source-detector pairs. When two readings are linearly combined, the weights of the two readings are either (1/2, 1/2) or (3/4, 1/4). In the latter case, the reading with a higher weight is shown boldface in the matrix of Fig. 2. When three readings are linearly combined, the weights are (1/2, 1/4, 1/4,) with the higher weighted reading shown in boldface. The individual pixel values have been linearly interpolated to produce the final optical maps. The small computation time required by this back-projection/linear interpolation scheme allows for the display of the optical images on-line during the measurement. Similar to the DPF method, our backprojection scheme is not expected to accurately quantify non-uniform absorption changes. Consequently, the micromolar values of $[\Delta HbO_2]$ and $[\Delta Hb]$ obtained with our DPF/backprojection approach is not quantitatively accurate in the presence of localized absorption changes.

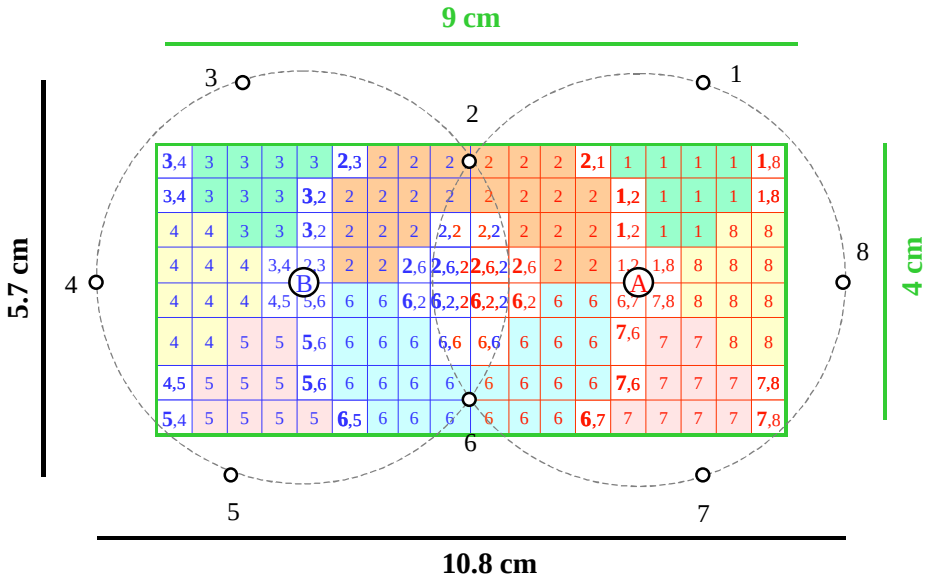

Fig. 2. Backprojection scheme used to generate the optical maps. The pixel size is 0.5×0.5 cm^2 The numbers in each pixel indicate the corresponding source location, while their colors indicate the detector (red for detector A, blue for detector B). Two or three numbers in one pixel indicate a linear interpolation of the corresponding readings. If one reading has a higher weight, it is indicated in boldface.

4. Measurement protocol

The measurement protocol consists of a periodic motor stimulation (hand tapping) performed by repeating a series of stimulation/rest sequences. The subject was a healthy, right-handed 20 year old male. The subject was comfortably lying on his back for the whole duration of the experiment. After a 10 min baseline acquisition, the subject was asked to tap with the right hand for 10 seconds, followed by 17 seconds of rest. This tapping/rest sequence was repeated

#18957 - $15.00 US
Received December 14, 1999; Revised January 19, 2000

ten times for a total measurement time of about 5 min. The frequency of hand-tapping was set by a metronome to 2.5 Hz. The optical probe was located on the subject's primary motor cortex, on the side contralateral to the tapping hand as illustrated in Fig. 1. The lower panel of Fig. 1 shows a portion of the measurement about 1.5 min long, which includes three hand-tapping periods (indicated by the blue bars) and four rest periods.

5. Results

During baseline acquisition, with the subject comfortably resting in a supine position, we have imaged the arterial pulsation. Figure 3(a) shows the maps of changes in oxy-hemoglobin concentration over a period of 1.6 s, which covers two heartbeat periods. The heart rate is about 77 min^{-1}, corresponding to a period of 780 ms. The acquisition time of 160 ms (about 1/5 of the heartbeat period in this case) gives us a sufficient temporal resolution to image the arterial pulsation. We have chosen the oxy-hemoglobin map because the arterial pulsation modulates the tissue concentration of arterial hemoglobin, which is almost fully oxygenated. Next to each optical image of the brain, we show the temporal trace of the arterial pulsation simultaneously recorded on a toe of the subject by the pulse oximeter. During the heartbeat period, one can clearly recognize the systolic (maximum [HbO_2]) and diastolic (minimum [HbO_2]) phases. We observe that the whole image oscillates in phase, but the amplitude of the [HbO_2] oscillation is spatially dependent. This may result from a spatial inhomogeneity in the distribution of the arteries. Figure 3(b) is a 15-s video of the spatially resolved arterial pulsation optically imaged on the subject's head.

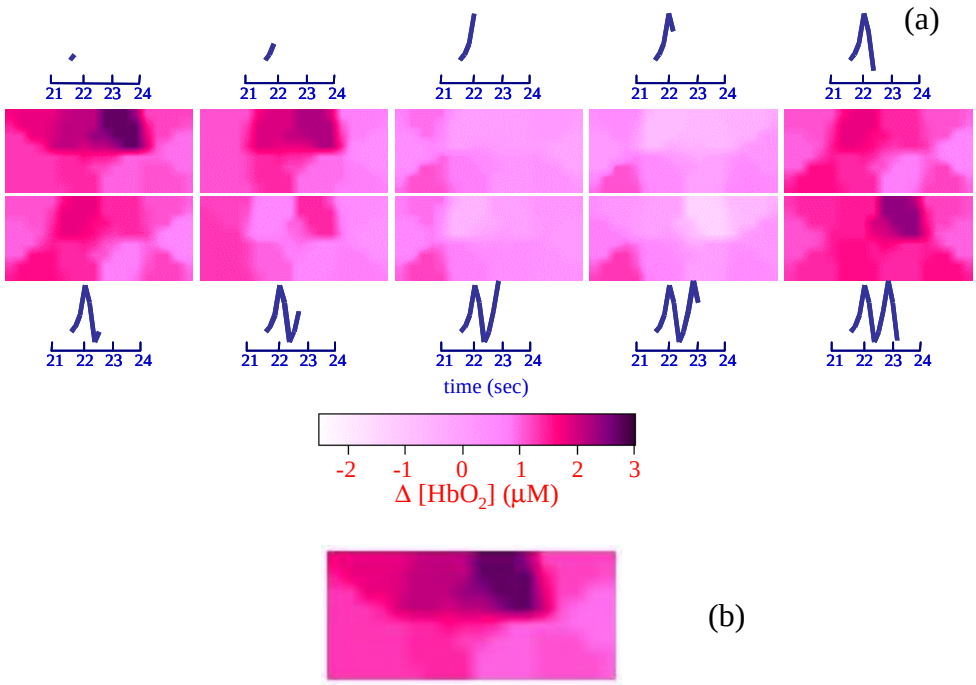

Fig. 3. (a) Oxy-hemoglobin optical maps of the brain over two heartbeat periods during baseline acquisition. The acquisition time is 160 ms. The traces next to each image are the pulsation readings from the pulse oximeter on a toe of the subject. (b) Real-time video of the spatial map of relative oxy-hemoglobin concentration during baseline (from t = 21.5 s to t = 36.5 s). The duration of the quicktime video is 15 s and the file size is 301 kB.

The experimental set-up for the hand-tapping protocol is schematically illustrated in Fig. 1. Figure 1 is also a real-time video of the optical brain image of relative deoxy-hemoglobin concentration (Δ[Hb]) during the hand tapping protocol. In addition to the image

#18957 - $15.00 US
Received December 14, 1999; Revised January 19, 2000

of cerebral Δ[Hb], this video schematically shows the location of the optical probe on the subject's head and the hand-tapping procedure. The temporal graph in the lower part of Fig. 1 shows the Δ[Hb] traces from two representative source-detector pairs, namely 1A and 6B. The latter (6B) is the source-detector pair that recorded the strongest response to motor activation, while the first one (1A) is about 5 cm away and did not record a significant deoxy-hemoglobin response to activation. In the optical monitoring of the cerebral response to hand tapping, we have filtered out the high frequencies related to the arterial pulsation by performing a running average over 800 ms (i.e. five frames). Consequently, we still display one image every 160 ms, but each image results from the average of the preceding five images. This is appropriate because the hemodynamic response to brain activation occurs over a time scale of seconds. The temporal traces of Δ[Hb] in Fig. 1 also serve the purpose of a temporal marker, indicating the progress of the measurement through the three tapping periods covered by the duration of the video. The three tapping periods shown here are the second, third and fourth ones of the ten periods that constitute the complete hand-tapping protocol. All of the ten tapping periods showed a similar response in the optical images.

Figure 1 shows the deoxy-hemoglobin image during the tapping protocol. Figure 4 compares the maps of oxy and deoxy-hemoglobin concentration changes measured at rest and at the maximum change in oxy-hemoglobin concentration during the fourth tapping period (t=68.5 s). Figure 4 is also the video of the maps of $\Delta[HbO_2]$ and Δ[Hb] for the same three successive periods of tapping and rest shown in Fig. 1. We observe that the color scale in the $\Delta[HbO_2]$ map is the same as in the arterial pulsation maps of Fig. 3.

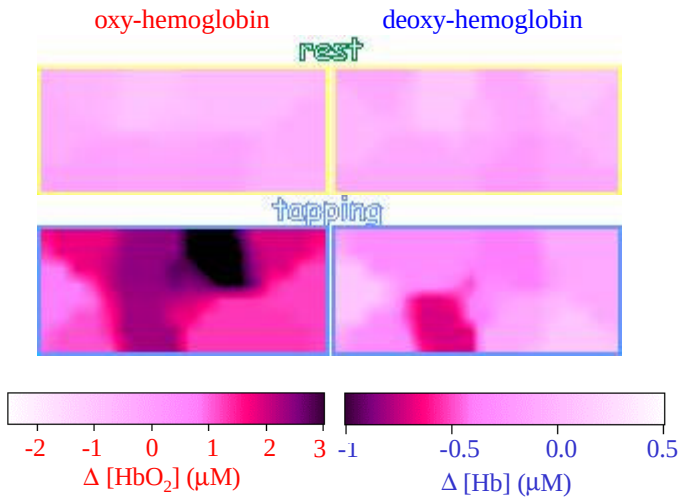

Fig. 4. Maps of oxy-hemoglobin (left panels) and deoxy-hemoglobin (right panels) changes at rest (top) and at the time of maximum response during the third tapping period (bottom). The top figure is a video of $\Delta[HbO_2]$ (left panel) and Δ[Hb] (right panel) during three successive rest/tapping periods. Note that the color scales for $\Delta[HbO_2]$ and Δ[Hb] are inverted (in the oxy-hemoglobin map, darker means an increase in concentration, while in the deoxy-hemoglobin map it means a decrease in concentration). This is done to produce the same visual effect for the opposite behavior of the two species during motor stimulation. The quicktime video duration is 86 s and the file size is 2,257 kB.

During hand tapping, there is a local increase in blood flow over the motor cortex area [28]. This activation-induced increase in blood flow determines a focal increase in oxy-hemoglobin concentration and a decrease in deoxy-hemoglobin concentration, as shown in

#18957 - $15.00 US
Received December 14, 1999; Revised January 19, 2000

Fig. 4. While our optical maps show a localized decrease in [Hb] during hand tapping, the cerebral [HbO_2] increases over a much larger area. In fact, we observed an increase in oxy-hemoglobin concentration over the whole imaged area, even though the amplitude of the increase was not spatially uniform. This suggests a systemic contribution to the oxy-hemoglobin signal. Figure 5 shows the time traces of oxy- and deoxy-hemoglobin concentrations for the duration of the video of Fig. 4. The oxy-hemoglobin traces are shown together with the optical signal recorded by the pulse oximeter on the foot of the subject. The fact that the systemic signal detected by the pulse oximeter well correlates with the oxy-hemoglobin signal on the brain explains the lack of localization observed in the oxy-hemoglobin map during motor stimulation. The systemic contribution to the cerebral hemodynamics strongly affects the oxy-hemoglobin concentration, and it superimposes with the focal oxy-hemoglobin change induced by motor activation.

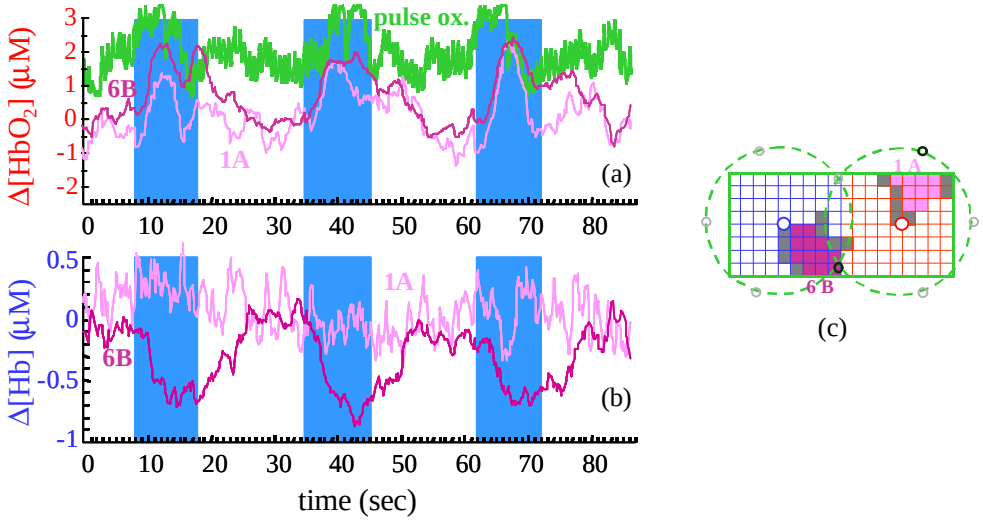

Fig. 5. (a) Oxy-hemoglobin and and (b) deoxy-hemoglobin concentration traces recorded with source-detector pairs 6B and 1A during the three rest/tapping periods shown in the videos of Figs. 1 and 4. The blue bars indicate the tapping periods. Panel (a) also shows the optical signal recorded by the pulse oximeter on a toe of the subject. (c) Geometrical arrangement of the optical probe with the indication of the zones probed by source-detector pairs 6B and 1A (see also Fig. 2).

6. Discussion

We have presented a non-invasive instrument for the real-time, on-line optical imaging of the human brain. The videos of Figs. 1, 3, and 4 illustrate the capabilities and the potential of this instrument. The observed difference in the localization of the activated cortex area in the oxy- and deoxy-hemoglobin images during motor stimulation (Fig. 4) confirms our recent findings in a study on five healthy subjects [29]. As suggested by Fig. 5, this result may be determined by a systemic contribution to the hemodynamics, which is synchronous with the motor stimulation task. The fact that this systemic contribution has a more significant effect on the [HbO_2] than on the [Hb] indicates that its origin may be in the almost fully saturated arterial hemoglobin compartment.

Our frequency-domain imaging system collects amplitude and phase data with the same temporal resolution as the intensity data. Here, we have only reported images of relative oxy- and deoxy-hemoglobin concentrations that are computed from spatially resolved intensity

#18957 - $15.00 US
Received December 14, 1999; Revised January 19, 2000

data. However, amplitude and phase data have the potential of providing additional useful information in optical imaging of the brain. In fact, phase information may be used to measure the local value of the DPF [26], rather than relying on literature values. However, the particular value of the DPF has little influence on the qualitative trend (increase vs. decrease) of the measured oxy- and deoxy-hemoglobin concentrations, whose measurement is the main objective of the imaging system reported here. Furthermore, the influence of the DPF value on the quantitation of Δ[Hb] and Δ[HbO_2] may be overwhelmed by the effect of spatial tissue inhomogeneities. In any case, an accurate measurement of the spectral dependence of the DPF (in our case, the ratio of the DPF values at the two wavelengths) may be important to minimize the cross-talk between Hb and HbO_2 [30]. G. Gratton *et al*. have reported that the phase signal can non-invasively detect fast neuronal activity signals with a latency of 50-100 ms [31]. We observe that, as a result of the multiplexing of the sixteen laser diodes, the optical data from the thirty-two source-detector pairs are acquired in series. Consequently, our backprojection algorithm may linearly combine readings that have been acquired at different times, the time difference ranging from 10 to 150 ms in our case. This would require a re-phasing of the individual source-detector readings for the accurate imaging of temporal processes on a 100 ms time scale or faster. Such a re-phasing was not necessary in the application reported here, as the arterial pulsation and the activation-induced cerebral hemodynamics occur on a time scale of seconds.

Our optical imaging approach is based on data measured with a collection of source-detector pairs. The data from each source-detector pair is highly sensitive to optical changes occurring at superficial tissue layers [32]. Consequently, extracranial hemodynamics gives a contribution to the optical signal that combines with the contribution from the cerebral cortex. This can be particularly important in the imaging of the arterial pulsation, where the capability of discriminating the extracranial and intracranial pulsatile contributions may result in a novel approach to the detection of strokes and cerebral hemorrhages. We observe that pressure-induced changes in the optical-fibers/skin coupling may also contribute to the pulsatile optical signal. However, by assuming that the hemoglobin in the arterial compartment gives the dominant contribution to the pulsatile optical signal, we have recently been able to accurately measure the arterial saturation [33]. For this reason, to generate Fig. 3, we have considered the pulsatile absorption as completely due to [Hb] and [HbO_2] changes.

7. Conclusion

We believe that to effectively investigate the optical signals collected on the brain under rest and stimulation conditions, it is important to combine the excellent temporal resolution that can be achieved with optical methods, with a spatially resolved measurement that provides imaging capabilities. This is the main objective of our optical imaging instrument. Furthermore, our backprojection approach allows for the real-time, on-line optical imaging of the brain, as demonstrated by the videos presented here. By increasing the number of source-detector channels, one can achieve more refined maps (smaller pixel size) of larger brain areas, to possibly cover the entire cerebral cortex. Real-time, on-line optical imaging of the entire human brain cortex with a temporal resolution in the 100 ms range can open new opportunities in human brain research.

Acknowledgments

This research is supported in part by the US National Institutes of Health (NIH) Grant No. CA57032, and by Whitaker-NIH Grant No. RR10966.

#18957 - $15.00 US Received December 14, 1999; Revised January 19, 2000